Robust Frequency Control in an Islanded Microgrid: H_∞ and μ-Synthesis Approaches

Hassan Bevrani, *Senior Member, IEEE*, Mohammad Ramin Feizi, *Student Member, IEEE*, and Sirwan Ataee, *Student Member, IEEE*

***Abstract*—This paper addresses robust frequency control in an islanded ac microgrid (MG). In an islanded MG with renewable sources, load change, wind power fluctuation, and sun irradiation power disturbance as well as dynamical perturbation, such as damping coefficient and inertia constants, can significantly influence the system frequency, and hence the MG frequency control problem faces some new challenges. In response to these challenges, in this paper, H_∞ and μ-synthesis robust control techniques are used to develop the secondary frequency control loop. In the proposed control scheme, some microsources (diesel engine generator, micro turbine, and fuel cell) are assumed to be responsible for balancing the load and power in the MG system. The synthesized H_∞ and μ-controllers are examined on an MG test platform, and the controllers' robustness and performance are evaluated in the presence of various disturbances and parametric uncertainties. The results are compared with an optimal control design. It is shown that the μ-synthesis approach due to considering structured/parametric uncertainties provides better performance than the H_∞ control method.**

***Index Terms*—Frequency control, H_∞, microgrid (MG), μ-synthesis, robust control, secondary control, uncertainty.**

NOMENCLATURE

BES	Battery energy storage.
D	Damping coefficient.
DEG	Diesel engine generator.
DER	Distributed energy resource.
DG	Distributed generator.
FES	Flywheel energy storage.
FC	Fuel cell.
LFT	Linear fractional transformation.
M	Inertia constant.
MG	Microgrid.
MGCC	MG central controller.
MT	Micro turbine.
NP, NS	Nominal performance and nominal stability.
PV	Photovoltaic panel.
WTG	Wind turbine generator.
RES	Renewable energy source.
RP, RS	Robust performance and robust stability.
ΔP_{DEG}	DEG output power change.
ΔP_{MT}	MT output power change.
ΔP_{FC}	FC output power change.
ΔP_{PV}	PV output power change.
ΔP_{BES}	BES output power change.
ΔP_{FES}	FES output power change.
ΔP_{φ}	Solar radiation power change.
ΔP_{Wind}	Wind power change.
ΔP_{L}	Load power change.
ΔP	Real-power unbalance.
Δf	Frequency deviation.
Δ	Uncertainty block.
T_{DEG}	DEG time constant.
T_{MT}	MT time constant.
T_{FC}	FC time constant.
T_{WTG}, T_{PV}	WTG and PV time constants.
T_{BES}, T_{FES}	BES and FES system time constants.
K_μ	μ-synthesis controller.
K_∞	H_∞ controller.

Manuscript received September 9, 2014; revised January 17, 2015 and May 2, 2015; accepted June 12, 2015. This work was supported by the Research Office at the University of Kurdistan. Paper no. TSG-00903-2014. *(Corresponding author: Hassan Bevrani.)*

The authors are with the Department of Electrical and Computer Engineering, University of Kurdistan, Sanandaj 6618614881, Iran (e-mail: bevrani@ieee.org).

Color versions of one or more of the figures in this paper are available online at http://ieeexplore.ieee.org.

Digital Object Identifier 10.1109/TSG.2015.2446984

I. INTRODUCTION

RECENTLY, remote off-grid MGs have been widely developed especially for rural and distant areas, in which providing electrical energy from the main utility grid is costly and has destructive environmental effects. There are many real MGs installed for providing the electrical energy for distant areas [1]–[4]. On the other hand, MGs control in an islanded mode is more difficult than the grid-connected mode, because voltage and frequency regulation of the MGs in grid-connected mode are initially supported by the main utility grid. In the islanded mode, some MG resources should compensate the fluctuation in load and generation (wind power and solar irradiation).

Low inertia, uncertainties, dynamic complexity, nonlinear structure, and intermittent nature of DER are the most important challenges in the MGs. Therefore, if a mismatch between the load and power generation occurs, the MG frequency and voltage deviation (from nominal value) is unavoidable, even it may lead to the MG blackout. Therefore, it seems that the robust control design strategies can be considered as a powerful solutions to achieve RS/RP in the presence of environmental condition and load deviation in the MGs [5], [6].

In the MGs, using distributed resources is essential. Distributed resources that mostly participate in the structure

of an MG are WTGs, DEGs, PVs, FCs, BES, and FES systems. Environmental and economic constraints are the main factors of choosing DERs for an islanded MG system. Since the produced power by RESs such as PVs and WTGs depends on the weather condition, the RESs are not preferred to be used for secondary frequency control. The MT and DEG units usually supply electrical energy for demand side to compensate the electrical energy deficiency. However, they have a slow response time and cannot handle MG control for sudden changes in load and power. So for improving the MT or DEG control efforts, coordination with energy storage systems is required to quickly compensate deviations [7]–[10].

Similar to the conventional power networks, a hierarchical control approach for MGs is proposed. Local/primary control, secondary control, and global/tertiary control are the most important control levels [10]–[12]. Robust control synthesis for secondary frequency regulation loop is the aim of this paper. The secondary control ensures that the set points of the MG are adapted to the optimality requirement of the MG and the frequency and average voltage deviations are regulated toward zero after any change in load or supply [13]. Two main structures have been identified for secondary control in MGs: 1) centralized and 2) decentralized structures. The centralized scheme relies on the operation of the MGCC and the decentralized scheme allows the interaction of the various units within the MG [14], [15]. Generally, the centralized structures are more suitable for islanded MGs, while decentralized schemes are more suitable for grid-connected MGs, with multiple owners and fast-changing number of DER units [14]. In this paper, a centralized approach is used.

In [16]–[19], some aspects of secondary control in MGs are investigated. In [16], a potential function is obtained for controllable units in the MG, and a central controller determines the set points, to optimize the overall performance of the MG. In comparison with [16], due to possibility of failure in the communication links, Shafiee *et al.* [17] did not build secondary control in the MGCC, so failure in a communication link does not affect the other distributed units and primary/secondary frequency controls are implemented as local controllers.

In [5], [6], and [19]–[21], several methods are applied to frequency control problem in MGs. In [5] and [19], metaheuristic optimization algorithms such as the Hopfield fuzzy neural network method and combined particle swarm optimization (PSO) with fuzzy logic are applied to regulate frequency deviation. In [20] and [21], to enhance the frequency control performance and robustness in the presence of uncertainties, the mixed H_2/H_∞ and PSO-based mixed H_2/H_∞ are proposed for tuning proportional–integral–derivative parameters. In [22], using a fuzzy-based proportional–integral (PI) control strategy, the stability of hybrid MG system, including MT, FC, and ES is investigated.

The applications of some classical and intelligent control methods are also reported in the MG control literature [5]–[22]. Using traditional control methods, it is not easy to achieve a successful tradeoff between NPs and RPs. It is also difficult to guarantee simultaneous RS and RP for a wide range of disturbances and uncertainties using the heuristic and intelligent control strategies. However, robust control techniques due to possibility of uncertainties formulation in the control synthesis procedure satisfy this objective effectively.

Because of considering physical constraints and uncertainties, the linear robust control techniques provide effective control synthesis methodologies for dynamical systems. But, most linear robust control methods suggest complex state-feedback controllers, whose orders are not smaller than the order of controlled systems [33], [35]. However, the small size of MGs in comparison with conventional large-scale power systems, once again directs our attention to use these powerful synthesis methodologies for the MGs control problems.

In [15] and [23]–[30], some studies on robust control applications for various MG systems are presented. In [15], a decentralized robust control strategy for an islanded MG is investigated. The MG consists of different DERs, and for each generation unit a robust controller is designed. In [26], for frequency regulation in an autonomous MG, a μ-based robust controller is proposed. The μ-synthesis robust controller is designed via the *D-K* iteration method. In [27] and [28], more works on μ-synthesis robust methods are presented. In [29], an H_∞ robust controller for power sharing in both interconnected and islanded modes is given. Similar works for utilizing H_∞ robust control strategies on the MGs are presented in [30] and [31].

In [15] and [23]–[30], the comparison between H_∞ and μ-synthesis applications in MG control is not given. The impacts of uncertainty modeling on the control performance are also not discussed.

This paper focuses on the application of H_∞ and μ-synthesis robust controls for improving secondary frequency control performance in an islanded MG. The proposed robust approaches are flexible enough to include uncertainties in the MG model and control synthesis procedure. For both H_∞ and μ methods, LFT is used. In the H_∞ control method, the parametric perturbation is lumped into one block as unstructured uncertainty; while in the μ-synthesis method, structured uncertainty is used. The RS and RP of both controllers are investigated.

The rest of this paper is organized as follows. Section II describes the MG modeling. In Section III, the state-space dynamical modeling is presented. The H_∞ method in order to obtain robust controller is investigated in Section IV. In Section V, the μ-synthesis technique is applied. Controller order reduction is presented in Section VI. Evaluating time-domain performance of H_∞ and μ-controllers on the MG secondary control and their comparison are presented in Section VII. Section VIII summarizes outcomes. Finally, the conclusion is presented in Section IX.

II. Microgrid Modeling

This paper focuses on the islanded ac MG including ac loads, WTG, PV, DEG, MT, FC, and energy storage devices such as FES and BES systems. Fig. 1 illustrates a simplified MG configuration. As shown in Fig. 1, distributed resources

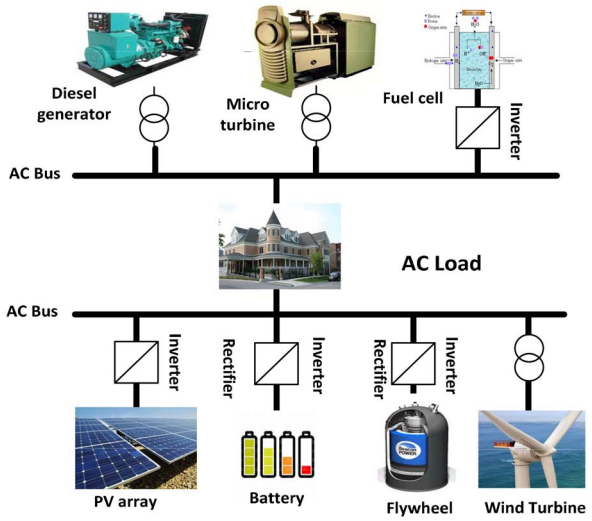

Fig. 1. Simplified schematic of an islanded MG.

are connected to the ac bus by power electronic devices used for synchronization of ac sources such as DEG and WTG, and they are used to invert dc voltages into ac in sources such as PV arrays and FCs. A converter is also considered for the BES system to convert ac to dc in charging mode and dc to ac in discharging mode.

The total power generation of distributed resources, for supplying demand side comprises the output power of DEG, MT, WTG, PV, FC, and exchange power of FES and BES

$$P_{\text{Load}} = P_{\text{DEG}} + P_{\text{MT}} + P_{\text{WTG}} + P_{\text{PV}} + P_{\text{FC}} \pm P_{\text{BES}} \pm P_{\text{FES}}. \tag{1}$$

Since, the produced power by the RESs such as PVs and WTGs depends on the environmental condition; they are not commonly used for frequency regulation, so in this paper, for secondary control problem, MT, DEG, and FC are considered. In secondary frequency control loop, the fluctuations in load, WTG, and PV output powers are compensated by decrease/increase in the DEG, MT, and FC output powers. An expression for changes in the MG resources associated with frequency regulation can be presented as follows:

$$\Delta P_{\text{Load}} + \Delta P_{\text{DEG}} + \Delta P_{\text{MT}} + \Delta P_{\text{FC}} + \Delta P_{\text{PV}} + \cdots \Delta P_{\text{WTG}} + \Delta P_{\text{BES}} + \Delta P_{\text{FES}} = 0. \tag{2}$$

In [19], [31], and [32], some simplified dynamical models for DGs/storage units are presented. Some distributed sources may have high-order dynamical frequency response models, but low-order dynamical models considered in this paper are sufficient for investigating frequency control issue [19]. Fig. 2 shows an MG dynamical frequency response model and the relevant system parameters for a typical MG are represented in Table I.

III. State Space Dynamic Model

Linearized state-space model is a useful model representation for the application of the robust control theory in the MG control synthesis. Using appropriate definitions and

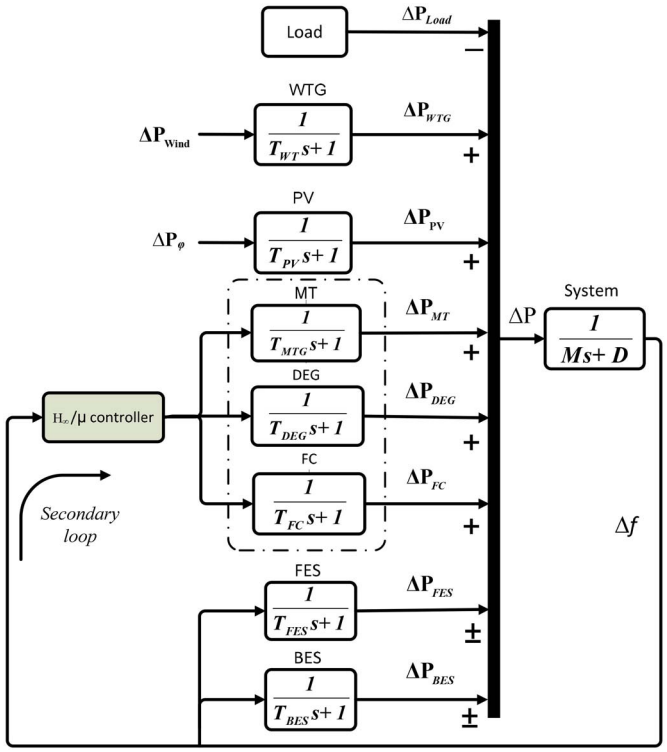

Fig. 2. MG dynamical frequency response model.

TABLE I
Parameters of Frequency Response Model (Fig. 2)

Parameter	Value	Parameter	Value
D (pu/Hz)	0.012	T_{DEG} (s)	2
M (pu/s)	0.2	T_{MT} (s)	2
T_{FC} (s)	4	T_{WTG} (s)	1.5
T_{BESS} (s)	0.1	T_{PV} (s)	1.8
T_{FESS} (s)	0.1		

state variables, as given in (3)–(6), the linearized state-space realization of the MG system (Fig. 2) can be easily obtained in the form of (3) [32]. An elaborated expression of the MG state-space model is given in (7) as shown at the bottom of the next page

$$\begin{aligned} \dot{x} &= Ax + B_1 w + B_2 u \\ y &= Cx \end{aligned} \tag{3}$$

where

$$x^T = \begin{bmatrix} \Delta P_{\text{WTG}} & \Delta P_{\text{PV}} & \Delta P_{\text{DEG}} & \Delta P_{\text{FC}} & \Delta P_{\text{MT}} & \Delta P_{\text{BES}} & \Delta P_{\text{FES}} & \Delta f \end{bmatrix} \tag{4}$$

$$w^T = \begin{bmatrix} \Delta P_{\text{Wind}} & \Delta P_{\varphi} & \Delta P_{\text{Load}} \end{bmatrix} \tag{5}$$

$$y = \Delta f \tag{6}$$

where u is the control input signal.

In the mentioned MG case study (Fig. 2), ΔP_{Wind}, ΔP_{φ}, and ΔP_{Load} are considered as MG disturbance signals and the M and D parameters are considered as uncertain parameters. More complete (higher order or nonlinear)

models of MG components for interested readers are given in [9], [18], [25], [29], [31], [37], and [38].

IV. H_∞-Based Control Design

The aim of this section is to design an H_∞-based controller for secondary frequency control loop in an islanded MG. The fundamentals of H_∞ control theory are briefly given in the Appendix.

A. Uncertainty Modeling

In robust control literature, several definitions for uncertainty modeling are represented [32], [33]; but in general, the uncertainty as dynamic perturbation can be mainly classified into two categories: 1) "unmodeled dynamics"; and 2) "modeling errors". The dynamic perturbations represent the difference between actual and mathematical models.

For H_∞-synthesis, dynamic parametric perturbations considered for the MG system are lumped into a single perturbation block $\Delta(s)$. This uncertainty representation is referred to as "unstructured uncertainty" [32], [33]. There are different methods for modeling unstructured uncertainty in robust control theory; such as additive perturbation, invers additive perturbation, and input/output multiplicative perturbation. In this paper, the output multiplicative perturbation method is used for uncertainty modeling.

Fig. 3 shows the block diagram of the closed-loop configuration which is used for the H_∞ design procedure. The lumped uncertainty and selected weighting functions are shown. $P(s)$ denotes the actual (perturbed system) dynamics, while $G(s)$ represents nominal model of the MG physical system without perturbation. As it can be seen from Fig. 3, the weighting functions $W_e(s), W_u(s), W_{d1}(s), W_{d2}(s)$, and $W_{d3}(s)$ are chosen to improve the RS and RP of system and $w_{\{1-3\}}, u, z_{\{1-5\}}$, and y are the exogenous disturbance inputs, control signals, desired performance signals, and measured output, respectively. A proper selection of the weighting functions is given

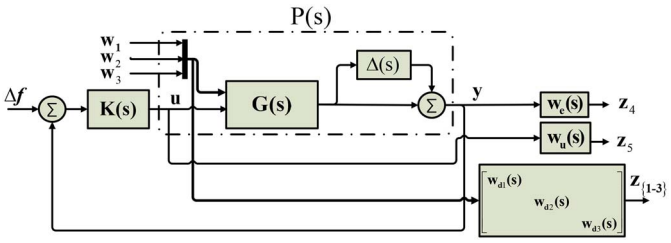

Fig. 3. Closed-loop system structure with lumped multiplicative uncertainty.

$$W_e(s) = 0.01\frac{s^3 + 5s^2 + 10s + 60}{s^3 + 100s^2 + 15s + 3} \tag{8}$$

$$W_u(s) = \frac{2(s+1)}{0.01s + 9} \tag{9}$$

$$W_d = \begin{bmatrix} 0.01 & & \\ & 0.01 & \\ & & 0.01 \end{bmatrix} = 0.01 I_{3\times 3}. \tag{10}$$

Considering $\pm 50\%$ deviations for D and M, bode diagram of output multiplicative perturbed system $P(s)$(with three disturbance inputs, one control input, and one measured output) is shown in Fig. 4. As mentioned, ΔP_{Wind}, ΔP_φ, and ΔP_{Load} are considered as MG disturbance signals and Δf is the measured system output. In Fig. 4, $T_{w1y}(j\omega)$, $T_{w2y}(j\omega)$, $T_{w3y}(j\omega)$, and $T_{uy}(j\omega)$ represent the system bode diagrams from the MG input signals (ΔP_{Wind}, ΔP_φ, ΔP_{L}, and control command) to output signal (Δf). These plots show the frequency response behavior for the perturbed input–output subsystems.

B. H_∞ Optimal Controller

The H_∞ controller is an optimization control problem, which determines a feasible robust controller by minimizing

$$\dot{x} = \begin{bmatrix} -1/T_{\text{WTG}} & 0 & 0 & 0 & 0 & 0 & 0 & 0 \\ 0 & -1/T_{\text{PV}} & 0 & 0 & 0 & 0 & 0 & 0 \\ 0 & 0 & -1/T_{\text{DEG}} & 0 & 0 & 0 & 0 & 0 \\ 0 & 0 & 0 & -1/T_{\text{FC}} & 0 & 0 & 0 & 0 \\ 0 & 0 & 0 & 0 & -1/T_{\text{MT}} & 0 & 0 & 0 \\ 0 & 0 & 0 & 0 & 0 & -1/T_{\text{BES}} & 0 & 1/T_{\text{BES}} \\ 0 & 0 & 0 & 0 & 0 & 0 & -1/T_{\text{FES}} & 1/T_{\text{FES}} \\ 0 & 0 & 0 & 0 & 0 & 0 & 0 & -2D/M \end{bmatrix} \begin{bmatrix} \Delta P_{\text{WTG}} \\ \Delta P_{\text{PV}} \\ \Delta P_{\text{DEG}} \\ \Delta P_{\text{FC}} \\ \Delta P_{\text{MT}} \\ \Delta P_{\text{BES}} \\ \Delta P_{\text{FES}} \\ \Delta f \end{bmatrix}$$

$$+ \begin{bmatrix} 1/T_{\text{WTG}} & 0 & 0 \\ 0 & 1/T_{\text{PV}} & 0 \\ 0 & 0 & 0 \\ 0 & 0 & 0 \\ 0 & 0 & 0 \\ 0 & 0 & 0 \\ 0 & 0 & 2/M \end{bmatrix} \begin{bmatrix} \Delta P_{\text{Wind}} \\ \Delta P_\varphi \\ \Delta P_{\text{Load}} \end{bmatrix} + \begin{bmatrix} 0 \\ 0 \\ 1/T_{\text{DEG}} \\ 1/T_{\text{FC}} \\ 1/T_{\text{MT}} \\ 0 \\ 0 \end{bmatrix} u, \quad y = \begin{bmatrix} 0 & 0 & 0 & 0 & 0 & 0 & 0 & 0 \end{bmatrix} x. \tag{7}$$

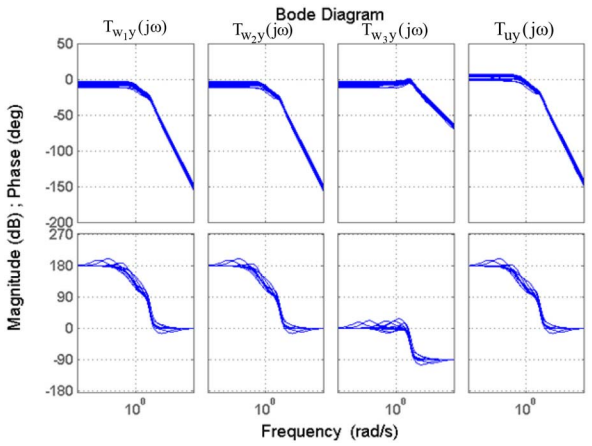

Fig. 4. Bode diagram of the perturbed system $P(s)$.

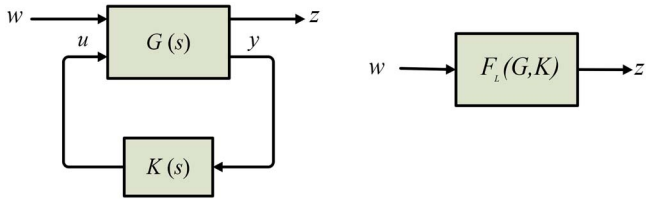

Fig. 5. H_∞ standard LFT configuration.

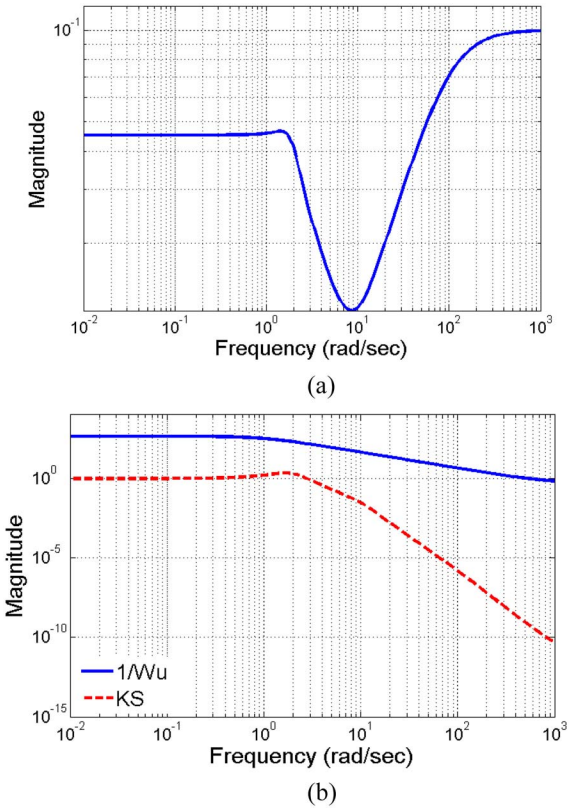

Fig. 6. (a) S and (b) KS functions of nominal system.

the infinite-norm of an appropriate LFT, $F_L(G, K)$, as follows:

$$\|F_L(G, K)\|_\infty < 1. \tag{11}$$

$F_L(G, K)$ is the transfer function matrix of the nominal closed-loop system from the disturbance input signals to the controlled output signals, which can be described as transfer function of T_{wz} [27]. There is no an analytic method for solving of above optimization problem. On the other hand, the solution for this minimization problem is not unique; so, it is usually sufficient to find a stabilizing controller K_∞ such that the H_∞-norm of (11) goes below one. Fig. 5 shows the standard closed-loop LFT for the H_∞ synthesis.

C. Closed-Loop Nominal Stability and Performance

The NS is satisfied because the closed-loop system T_{wz} is internally stable for the designed K_∞. For evaluating the NP, the infinity-norm of both sensitivity function $S = (I + GK)^{-1}$ and complementary function KS should be less than a positive value. The NP criterion for the closed-loop system can be described by (12) [21], [23], where W_e and W_u are weighting functions represented in (8) and (9)

$$\left\| \begin{bmatrix} W_e(I + GK)^{-1} \\ W_P K(I + GK)^{-1} \end{bmatrix} \right\|_\infty < 1. \tag{12}$$

Fig. 6 shows that the ∞-norm inequality of (12) is satisfied and is always less than one. So the closed-loop system successfully reduces the influence of the disturbance, and the required performance is fully achieved. In this paper, the *hinfsyn* command in MATLAB robust control toolbox is used for solving the above inequality.

D. Closed-Loop Robust Stability and Performance

The RS is satisfied because the closed-loop system (T_{wz} transfer function) is internally stable for all possible plants $P = (I + \Delta(s))G(s)$ in which the block Δ is the uncertainty block. For analyzing the RP, the performance criterion given in (13) must be satisfied for all $P = (I + \Delta(s))G(s)$. In this paper, T_{wz} function in the presence of 50% perturbations in D and M parameters is investigated. As shown in Fig. 7, the ∞-norm inequality represented in (13) is less than one

$$\left\| \begin{bmatrix} W_e(I + GP)^{-1} \\ W_P K(I + GP)^{-1} \end{bmatrix} \right\|_\infty < 1. \tag{13}$$

Fig. 7(a) shows that the inequality $\|[W_e(I+GP)^{-1}]\|_\infty < 1$ for $P = (I + \Delta(s))G(s)$ is always satisfied. Fig. 7(b) shows that the inequality $\|[W_P K(I+GP)^{-1}]\|_\infty < 1$ is also satisfied, or $\|[K(I+GP)^{-1}]\|_\infty$ is less than $1/W_P$. Therefore, the RS and RP are simultaneously satisfied for the obtained controller K via a single ∞-norm inequality which is represented in (13).

V. μ-Based Control Synthesis

The basics of structured singular value (μ) theorem are briefly given in the Appendix.

A. Uncertainty Modeling in μ-Synthesis

In Section IV, the uncertainties are modeled in a lumped block Δ, which refers to the "unstructured uncertainties." This type of uncertainty provides conservative results in the synthesis procedure. For solving this problem, the "structured

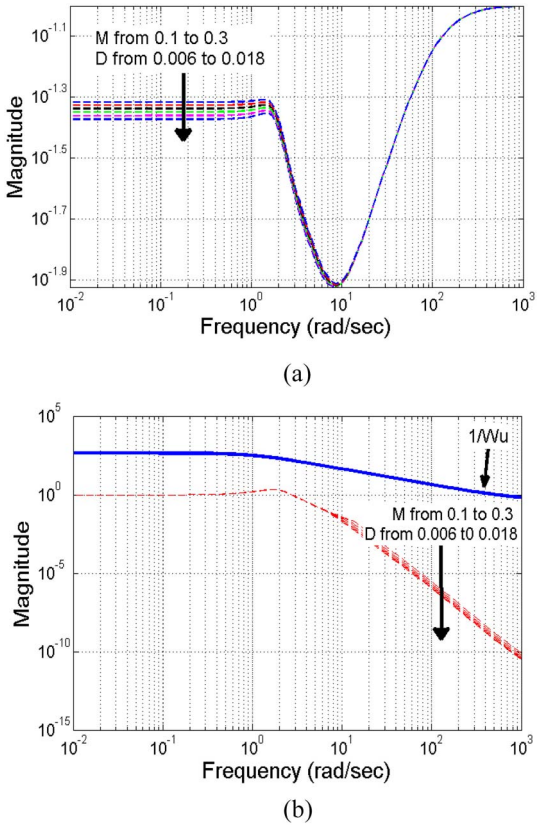

Fig. 7. (a) S and (b) KS functions in the presence of perturbations (RP).

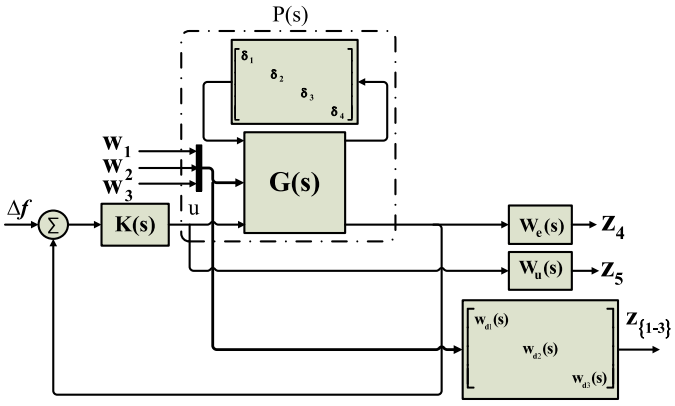

Fig. 8. Closed-loop system diagram with structured diagonal uncertainty block.

uncertainty" should be used [21]. The structured uncertainty may include structured unmodeled dynamics and parametric perturbation.

The structured uncertainty block Δ that is represented in the general form of (14) can be extracted from the system dynamics. So the whole system can be rearranged in a standard configuration of upper LFT. Fig. 8 shows the closed-loop block diagram of the MG system with a structured diagonal uncertainty. In this paper, the system has a 4×4 parametric diagonal uncertainty as shown in Fig. 8

$$\Delta = \Big\{\text{diag}\Big[\delta_1 I_{r1}, \ldots, \delta_k I_{rk}, \Delta_1, \ldots, \Delta_f\Big], \quad \delta_i \in C, \Delta_j \in C^{k_i \times k_j}\Big\}. \tag{14}$$

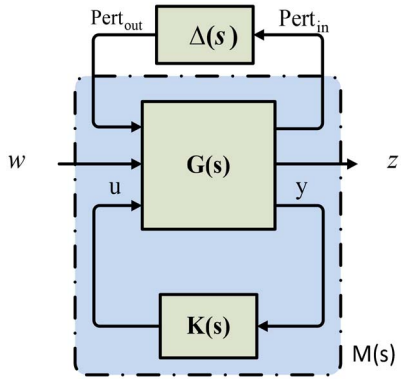

Fig. 9. Standard M-Δ configuration for μ-synthesis.

B. D-K Iteration

The structured singular value (μ-based control) framework provides conditions to ensure the RP of a dynamic system. The μ function is defined as (15), where Δ is defined as (14)

$$\mu_\Delta(M) = \frac{1}{\min\limits_{\Delta}\{\bar{\sigma}(\Delta) : |I - M\Delta| = 0, \Delta \in \Delta\}}. \tag{15}$$

The standard scheme of M-Δ configuration is shown in Fig. 9. The w, u, z, y, pert_{in}, and pert_{out} are the exogenous inputs, control signals, control performance signals, measured outputs, input, and output perturbations signals of the uncertain block, respectively. In μ-synthesis, for satisfying the RP condition, $\|T_{wz}\|_\infty \leq 1$ must be satisfied for all $\Delta \in \Delta_P$, where Δ_P is defined as follows:

$$\Delta_p := \left\{\begin{bmatrix}\Delta & 0\\ 0 & \Delta_F\end{bmatrix} : \Delta \in R^{4\times 4}, \Delta_F \in C^{4\times 5}\right\}. \tag{16}$$

The first uncertainty block Δ of this structured matrix is a 4×4 diagonal matrix and corresponds to the perturbations used in the dynamical modeling of islanded MG system. The second block Δ_F is a fictitious uncertainty block that is introduced to represent the performance requirement in the M-Δ framework. To achieve RP, the stabilizing controller $K(s)$ should minimize

$$\max_{\omega} \mu_{\Delta_p}(M(s)). \tag{17}$$

There is no standard analytical method to calculate the μ-optimal controller via the optimization problem given in (17). Therefore, a numerical method for complex perturbation known as D-K iteration [32] is used to solve (17). The idea is to find a controller K such that (18) be satisfied by alternating the minimization with respect to K or D, while fixing the other one

$$\min_K\left(\min_{D(j\omega)}\left\|D(j\omega)M(K(j\omega))D^{-1}(j\omega)\right\|_\infty\right). \tag{18}$$

Fig. 10 shows the simplified LFT configuration for implementing the D-K iteration method in order to design robust μ controller for the uncertain MG system using MATLAB toolbox. The iteration for designing μ controller with the D-K iteration method includes the following main steps.

1) *K-Step:* Synthesize an H_∞ controller for the scaled problem $\min \|D(s)M(K)D^{-1}(s)\|_\infty$, while $D(s)$ is fixed.

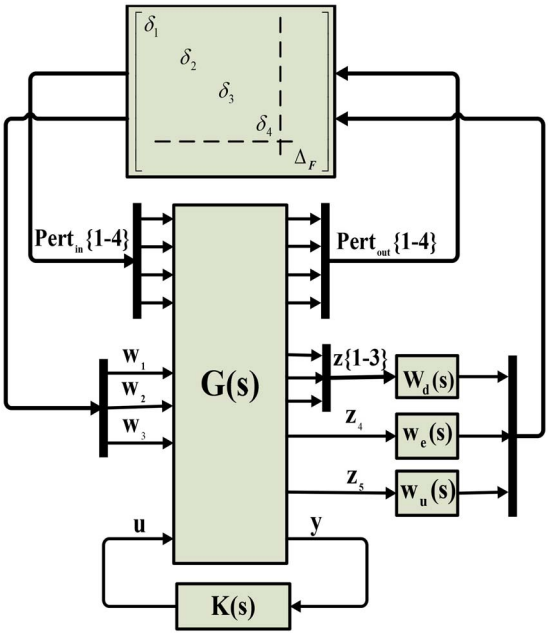

Fig. 10. Closed-loop configuration for using the *D-K* iteration method.

2) *D-Step:* Find $D(j\omega)$ to minimize $\overline{\sigma}(DM(K)D^{-1}(j\omega))$ over the given frequency range, while M (K) is fixed.
3) Fit the magnitude of each element $D(j\omega)$ to a stable and minimum-phase transfer function $D(s)$. Then, go back to step i.

These iterations continue until the $\|D(s)M)(K)D^{-1}(s)\|_\infty$ goes less than one or until the ∞-norm no longer decreases.

RP characteristics are extremely depends on appropriate selection of weighting functions. To have a better comparison between H_∞ and μ-synthesis methods, the same weighting functions are considered in both syntheses approaches.

C. Closed-Loop Nominal and Robust Performance

After designing K using the *D-K* iteration method, the maximum value of μ for RP is obtained: 0.57. To guarantee the RP with the obtained controller, the performance criterion (19) should be satisfied (infinity norm to be smaller than the upper bound of μ). Fig. 11 shows that the frequency response of NP and RP for the closed-loop system is satisfied. It is noteworthy that $||\Delta||_\infty<1$, for every diagonal Δ

$$\left\| \begin{bmatrix} W_e\big(I + F_U(G,\Delta)K^{-1}\big) \\ W_P K\big(I + F_U(G,\Delta)K^{-1}\big) \end{bmatrix} \right\|_\infty < 1. \qquad (19)$$

Fig. 12 shows the RP index for perturbed system sensitivity function. It is clear from this figure that the frequency response of dynamical perturbed MG system remains below 0.57.

D. Robust Stability

The upper and lower bounds of μ for the perturbed system are shown in Fig. 13. It is visible that the upper bound of μ is 0.922, so if the $||\Delta||_\infty < 1/0.922$, the RS for the perturbed closed-loop system is achieved, and $||\Delta||_\infty < 1$ is satisfied. Fig. 14 demonstrates the robust properties of system with the designed μ-controller. It is shown that the magnitude response

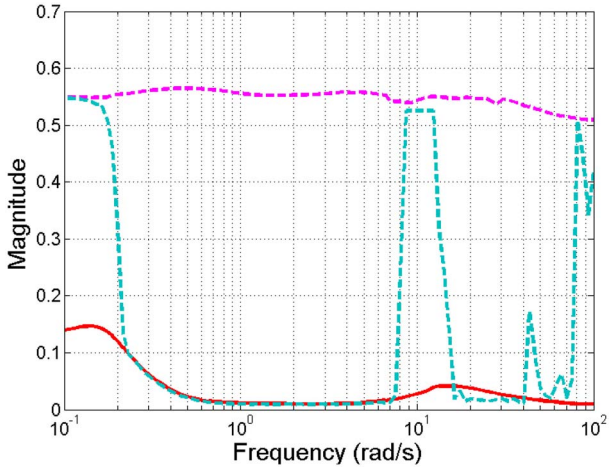

Fig. 11. NP (solid) and RP (dashed).

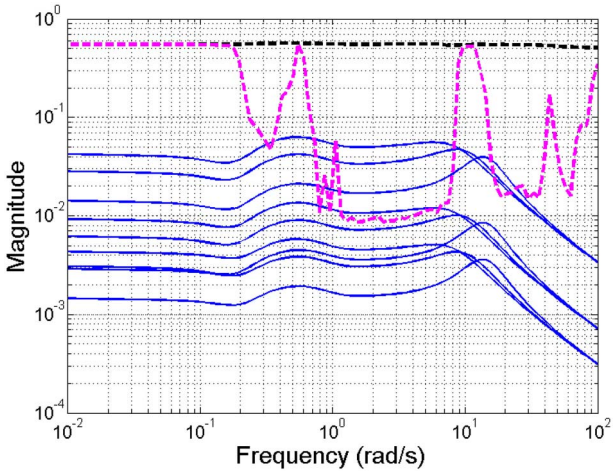

Fig. 12. RP index of perturbed systems (solid) and μ upper and lower bounds of perturbed closed-loop (dashed).

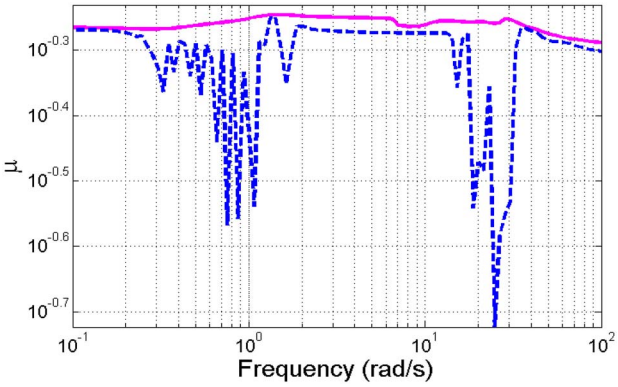

Fig. 13. RS of K, upper bound (solid), and lower bound (dashed).

of the perturbed sensitivity function over the given frequency range is below the magnitude of the inverse of weighting function W_e.

VI. Controller Order Reduction

High-order of designed controllers is one of the main problems of H_∞- and μ-based robust control methods, especially

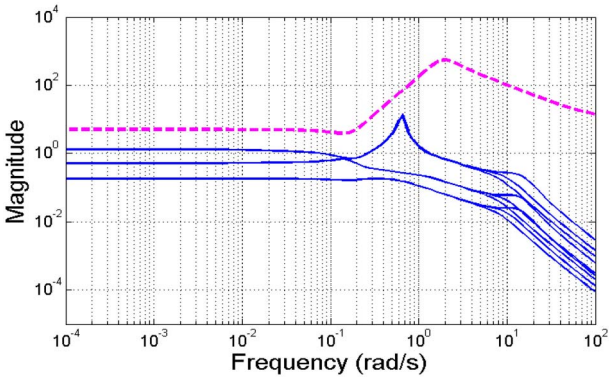

Fig. 14. Sensitivity functions of perturbed systems with K (solid) and W_e^{-1} (dashed).

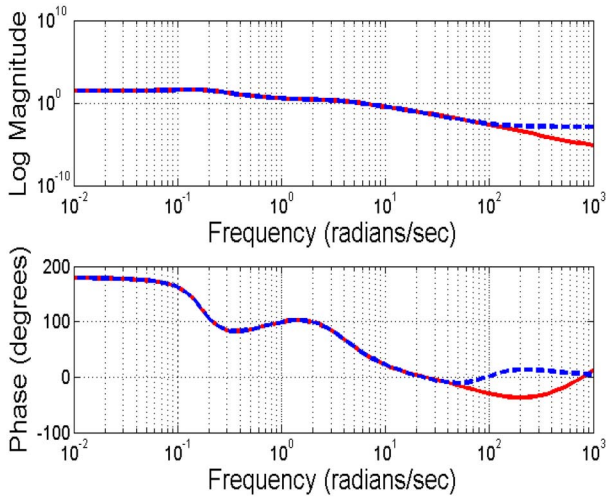

Fig. 15. Comparison between original (solid) and reduced-order (dashed) H_∞-controller.

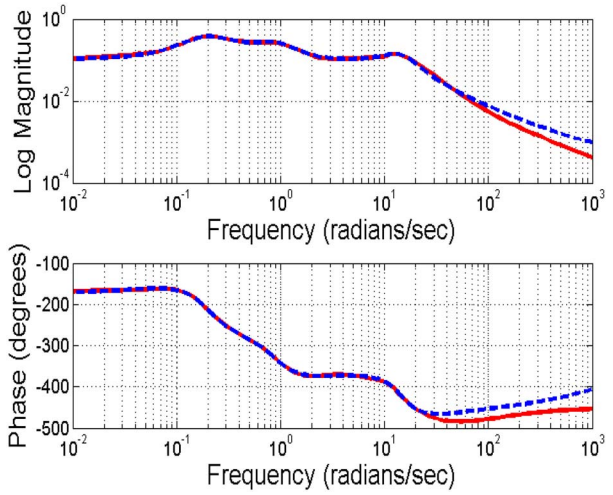

Fig. 16. Comparison between original (solid) and reduced-order (dashed) μ-controller.

for the high-order plants. Using these control methodologies, the obtained controller are higher than or at least equal with the order of the given plants. Different methods are introduced for order reduction. Here, for the present case study,

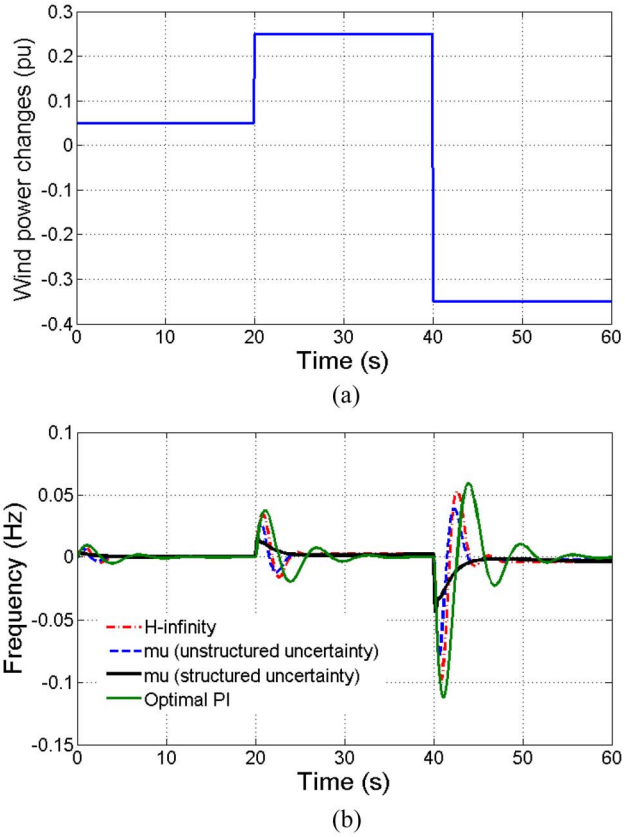

Fig. 17. (a) Wind power change pattern. (b) MG output frequency.

the Hankel-norm approximation [34] is applied to reduce the controller order.

The obtained controller order, by the H_∞ method was 14, which is reduced to 6. Fig. 15 shows the Bode diagram of full-order (original) and reduced-order for the H_∞ controller. After three iterations in the D-K method, the μ-synthesis controller order is 28, which is reduced to 7, using the Hankel-norm approximation method. In Fig. 16, the Bode diagrams of full-order and reduced-order controllers are demonstrated. Figs. 15 and 16 show that the resulting high-order controllers are reduced to low orders without performance degradation.

VII. Time-Domain Simulation Results

In this section, the time-domain simulation of MG frequency, in the presence of ΔP_{Wind}, ΔP_φ, and ΔP_{L} changes (as disturbances) and parameters perturbation is presented. The H_∞ method and μ-synthesis (with structured and unstructured uncertainties) are compared. To show the effectiveness of the proposed robust approaches, they are also compared with an optimal PI controller. The PI parameters are determined using the internal model control (IMC) design method. The IMC approach allows the designer to consider modeling errors and desirable performance, simultaneously [35]. For a given system, the applied tuning algorithm optimally balances the two measures of performance, reference tracking and disturbance rejection; concerning the system changes and modeling errors. For investigating the MG frequency response, four sever test scenarios are performed.

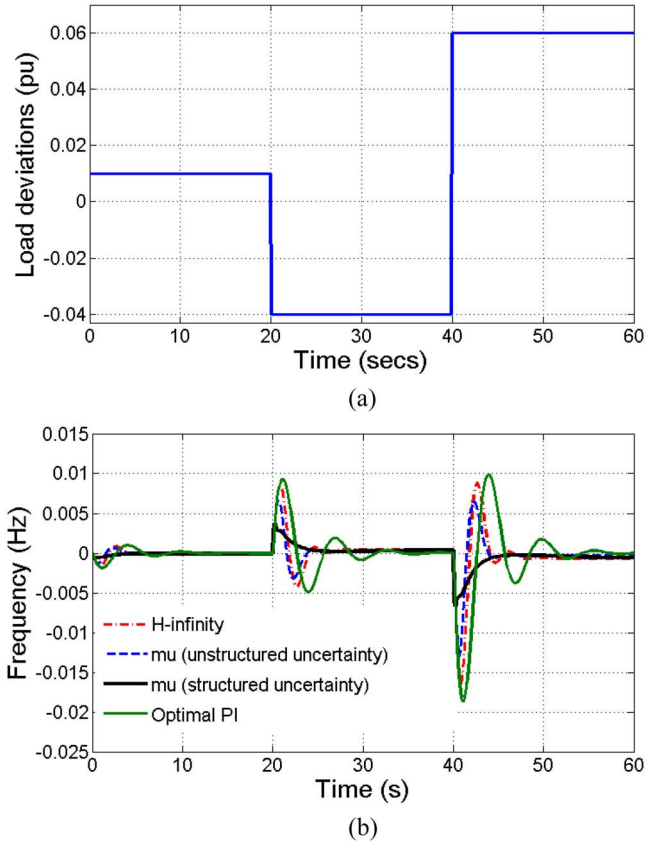

Fig. 18. (a) Multiple load deviation. (b) MG output frequency.

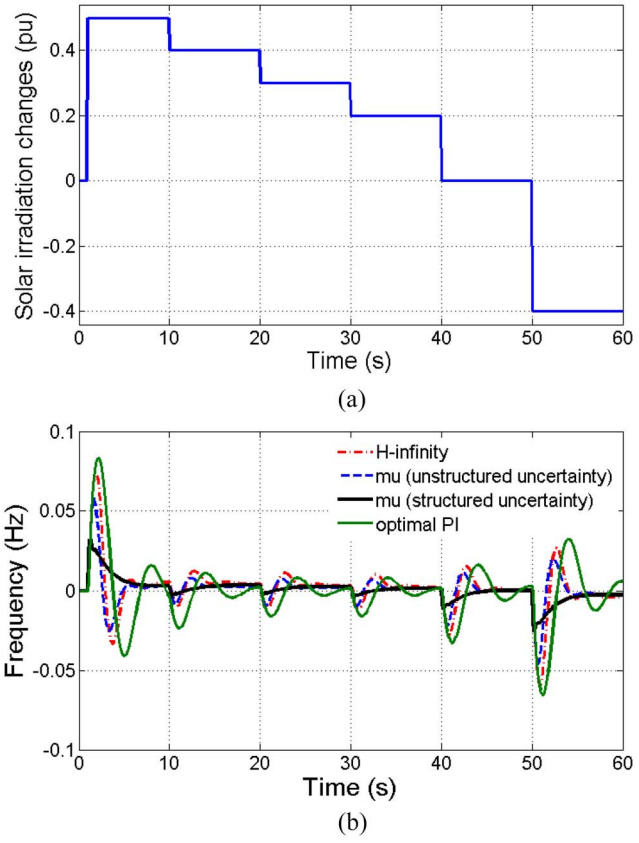

Fig. 19. (a) Solar power change pattern. (b) MG output frequency.

Scenario 1 [Wind Power Fluctuation (ΔP_{Wind})]: A step change is considered in the wind power. Fig. 17(a) shows the wind power step changes and Fig. 17(b) represents the MG output frequency response by comparing the proposed controllers.

Scenario 2 [Load Fluctuation (ΔP_{Load})]: A multiple step load deviation is considered with changes at times 0, 20, and 40 s. Fig. 18(a) shows the multiple load step change pattern. Fig. 18(b) represents the MG frequency response by comparing between the performance of the H_∞ controller and μ-controller (with structured and unstructured uncertainty).

Scenario 3 [Solar Power Fluctuation (ΔP_φ)]: As another serious test, a multiple step changes in the sun irradiation power is applied at times 1, 10, 20, 30, 40, and 50 s as shown in Fig. 19(a). Fig. 19(b) represents the MG frequency for the designed controllers.

Scenario 4 (Simultaneous Changes in ΔP_{Wind}, ΔP_φ, ΔP_{Load}, and MG Parameters): In this scenario, firstly simultaneous disturbances in wind power, sun irradiation power, and load are considered. Fig. 20(a) shows the mixed changes in wind power, solar irradiation, and load. Fig. 20(b) shows the MG frequency response behavior. Fig. 21(b) shows the system response for a more smooth and non-stationary fluctuation pattern [36] in solar irradiation and wind powers in the presence of step load variation as depicted in Fig. 21(b).

Then, the MG frequency response in the face of 50% decrease in H and D parameters (as uncertainties) is examined. The results are shown in Fig. 22. As demonstrated in Fig. 22, for this test scenario, the PI controller fails and cannot stabilize the MG frequency. While, in all scenarios, the proposed H_∞ and μ-synthesis approaches provide quite better performance.

Simulation results show that μ-controller with structured uncertainty gives quite better performance than the case of μ-controller with unstructured uncertainty as well as the H_∞ controller because the uncertainties in the MGs are of parametric/structured type; and hence using an unstructured uncertainty-based control technique provides nonexact conservative result.

VIII. Discussion

Functional complexity, diversity in generation/load, variable nature of RESs, and continues change of structure (uncertainty) are known as some important characteristics of the MGs. As shown in this paper, conventional controls may fail to meet the specified frequency control objective in the MGs. The above characteristics introduce robust control techniques as powerful and more suitable control tools for stability analysis and control synthesis problems in MGs and modern power grids.

The achievements of this paper are not only limited to the applications of H_∞ and μ-synthesize control techniques for the MGs' secondary frequency control design. The main outcomes can be summarized as follows.

1) Although the H_∞ and μ-synthesis approaches have been already applied to the power system. But as discussed in [32], only few applications are related to the MGs.

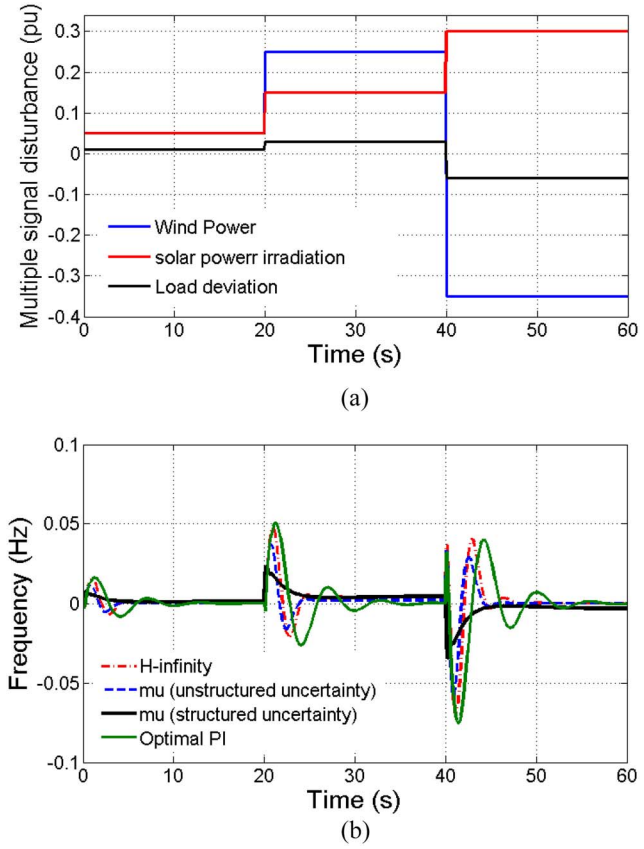

Fig. 20. (a) Multiple disturbances in load, wind speed, and solar irradiation. (b) MG output frequency.

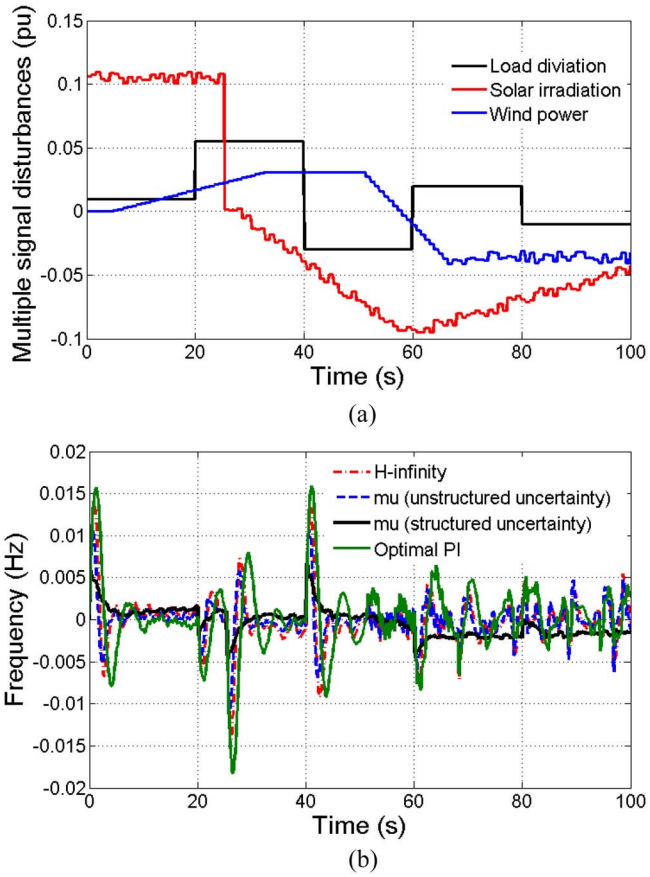

Fig. 21. (a) Multiple disturbances in load, wind speed, and solar irradiation. (b) MG output frequency.

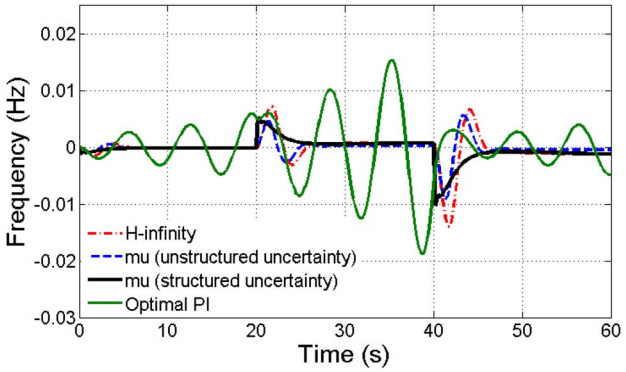

Fig. 22. MG output frequency in the presence of 50% uncertainty in H and D parameters and disturbance signal in Fig. 20(a).

Dynamics, generation, and load characteristics in MGs may be different from the conventional power grids. Hence, the application of a robust control theorem cannot be so easy and straightforward. On the other hand, in the previous published works, only one robust method is discussed; while in this paper, a comprehensive/precisely comparison between H_∞ and μ-synthesize methods is given and their advantages and disadvantages for the frequency control issue are clarified.

2) The type of most effective uncertainties in the MGs, that is structured and parametric uncertainties, is investigated. It is shown that the uncertainties in an MG can be modeled as structured/parametric type, and this investigation opens the way to use this paper as a reference for further research works on robust MG control. In direction of this achievement, the impact of uncertainty modeling is illustrated, and the superiority of structured/parametric-based control theory such as μ-synthesize for MG control is emphasized. It is shown that the structured/parametric-based robust control strategy dramatically increases the regulation performance and control accuracy.
3) Finally, simultaneously considering load change, various power fluctuations, and uncertainties in the MG frequency control problem among a single control framework/formulation via a systematic design approach can also be considered as a significant outcome of this paper.

IX. Conclusion

In this paper, robust H_∞ and μ-synthesis (via D-K iteration) methods are used for secondary frequency control design problem in an islanded MG. For applying robust control methods, linearized MG state-space model is derived. As discussed, using robust controllers provides many benefits. The H_∞ and μ-controllers are designed in a way to reduce the effects of ΔP_{Wind}, ΔP_φ, and ΔP_{Load} disturbances and dynamic perturbations. It is shown that in the case of using the structured uncertainty (μ approach), the obtained controller demonstrates better performance. Time-domain simulation results show the

proposed controllers can balance the power generation and load properly, and regulate the MG frequency effectively. Due to the use of structured uncertainties, μ-controller has better performance than the H_∞ controller. The order of original robust controllers is reduced. In comparison with optimal PI controllers, the application of robust reduced-order controllers dramatically improves the MG frequency control performance.

APPENDIX

Here, the basics of H_∞ and structured singular value (μ) theorems are briefly given. Interested readers can find details and proofs in [32].

A. H_∞ Control Theory

Consider a linear time invariant system $G(s)$ with the following state-space realization:

$$\begin{aligned} \dot{x} &= Ax + B_1 w + B_2 u \\ z &= C_1 x + D_{12} u \\ y &= C_2 x \end{aligned} \tag{A.1}$$

where x is the state variable vector, w is the disturbance and other external input vector, z is the controlled output vector, and y is the measured output vector.

It is assumed that (A, B_2, C_2) is stabilizable and detectable. The H_∞ control problem for the linear time invariant system $G(s)$ with the state-space realization of (A.1) is to find a controller $K(s)$ such that the resulted closed-loop system is internally stable, and the ∞-norm from w to z is smaller than γ, a specified positive number, that is

$$||T_{wz}(s)||_\infty < \gamma. \tag{A.2}$$

Using matrix representation, the K is a dynamic H_∞ controller, if and only if there exists a symmetric matrix $X > 0$ such that

$$\begin{bmatrix} A_{cl}^T X + X A_{cl} & X B_{cl} & C_{cl}^T \\ B_{cl}^T X & -\gamma I & D_{cl}^T \\ C_{cl} & D_{cl} & -\gamma I \end{bmatrix} < 0 \tag{A.3}$$

where

$$\begin{aligned} A_{cl} &= A + B_2 K C_2, \quad & B_{cl} &= B_1 \\ A_{cl} &= A + B_{12} K C_2, \quad & D_{cl} &= 0. \end{aligned}$$

B. Structured Singular Value (μ) Control Theory

Based on the μ-synthesis theorem, for a given M-Δ configuration (Fig. 9) the RS/RP is satisfied by controller $K(s)$ if and only if

$$\inf_K \sup_{\omega \in R} \mu\big[M(j\omega)\big] < 1 \tag{A.4}$$

where μ concept is represented in (15). Considering the upper bound of μ, the robust synthesis problem (A.4) can be reduced to determine

$$\min_K \inf_D \sup_{\omega \in R} \bar{\sigma}\left[DM(j\omega)D^{-1}\right] \tag{A.5}$$

or equivalently

$$\min_{K,D} \left\| DM(G(j\omega), K(j\omega))D^{-1} \right\|_\infty \tag{A.6}$$

by iteratively solving for D and K. Here, D is a positive definite symmetric matrix with appropriate dimension and $\bar{\sigma}(\cdot)$ denotes the maximum singular value of a matrix.

REFERENCES

[1] W. Al-Saedi, S. W. Lachowicz, D. Habibi, and O. Bass, "Power quality enhancement in autonomous microgrid operation using particle swarm optimization," *Int. J. Elect. Power Energy Syst.*, vol. 42, no. 1, pp. 139–149, 2012.

[2] J. Dekker, M. Nthontho, S. Chowdhury, and S. P. Chowdhury, "Economic analysis of PV/diesel hybrid power systems in different climatic zones of South Africa," *Int. J. Elect. Power Energy Syst.*, vol. 40, no. 1, pp. 104–112, 2012.

[3] G. D. Kamalapur and R. Y. Udaykumar, "Rural electrification in India and feasibility of photovoltaic solar home systems," *Int. J. Elect. Power Energy Syst.*, vol. 33, no. 3, pp. 594–599, 2011.

[4] J. A. Alzola *et al.*, "Microgrids project, Part 2: Design of an electrification kit with high content of renewable energy sources in Senegal," *Renew. Energy*, vol. 34, no. 10, pp. 2151–2159, 2009.

[5] W. Gu, W. Liu, Z. Wu, B. Zhao, and W. Chen, "Cooperative control to enhance the frequency stability of islanded microgrids with DFIG-SMES," *Energies*, vol. 6, no. 8, pp. 3951–3971, 2013.

[6] I. Şerban and C. Marinescu, "Aggregate load-frequency control of a wind-hydro autonomous microgrid," *Renew. Energy*, vol. 36, no. 12, pp. 3345–3354, 2011.

[7] T. Goya *et al.*, "Coordinated control of energy storage system and diesel generator in isolated power system," *Int. J. Emerg. Elect. Power Syst.*, vol. 12, no. 1, pp. 925–930, 2011.

[8] H. Bevrani, M. Watanabe, and Y. Mitani, *Power System Monitoring and Control*. Hoboken, NJ, USA: Wiley, Jun. 2014.

[9] S. Adhikari and F. Li, "Coordinated V-f and P-Q control of solar photovoltaic generators with MPPT and battery storage in microgrids," *IEEE Trans. Smart Grid*, vol. 5, no. 3, pp. 1270–1281, May 2014.

[10] J. M. Guerrero, P. C. Loh, T.-L. Lee, and M. Chandorkar, "Advanced control architectures for intelligent microgrids—Part II: Power quality, energy storage, and AC/DC microgrids," *IEEE Trans. Ind. Electron.*, vol. 60, no. 4, pp. 1263–1270, Apr. 2013.

[11] J. M. Guerrero, J. C. Vasquez, J. Matas, L. G. de Vicuña, and M. Castilla, "Hierarchical control of droop-controlled AC and DC microgrids—A general approach toward standardization," *IEEE Trans. Ind. Electron.*, vol. 58, no. 1, pp. 158–172, Jan. 2011.

[12] H. Bevrani, M. Watanabe, and Y. Mitani, "Microgrid controls," in *Standard Handbook for Electrical Engineers*. New York, NY, USA: McGraw-Hill, 2012.

[13] I. Ngamroo, "Application of electrolyzer to alleviate power fluctuation in a stand alone microgrid based on an optimal fuzzy PID control," *Int. J. Electr. Power Energy Syst.*, vol. 43, no. 1, pp. 969–976, 2012.

[14] D. E. Olivares *et al.*, "Trends in microgrid control," *IEEE Trans. Smart Grid*, vol. 5, no. 4, pp. 1905–1919, Jul. 2014.

[15] A. H. Etemadi, E. J. Davison, and R. Iravani, "A decentralized robust control strategy for multi-DER microgrids—Part I: Fundamental concepts," *IEEE Trans. Power Del.*, vol. 27, no. 4, pp. 1843–1853, Oct. 2012.

[16] A. Mehrizi-Sani and R. Iravani, "Potential-function based control of a microgrid in islanded and grid-connected modes," *IEEE Trans. Power Syst.*, vol. 25, no. 4, pp. 1883–1891, Nov. 2010.

[17] Q. Shafiee, J. M. Guerrero, and J. C. Vasquez, "Distributed secondary control for islanded microgrid—A novel approach," *IEEE Trans. Power Electron.*, vol. 29, no. 2, pp. 1018–1031, Feb. 2014.

[18] A. Bidram, A. Davoudi, F. L. Lewis, and J. M. Guerrero, "Distributed cooperative secondary control of microgrids using feedback linearization," *IEEE Trans. Power Syst.*, vol. 28, no. 3, pp. 3462–3470, Aug. 2013.

[19] H. Bevrani, F. Habibi, P. Babahajyani, M. Watanabe, and Y. Mitani, "Intelligent frequency control in an AC microgrid: Online PSO-based fuzzy tuning approach," *IEEE Trans. Smart Grid*, vol. 3, no. 4, pp. 1935–1944, Dec. 2012.

[20] S. Vachirasricirikul and I. Ngamroo, "Robust controller design of micro-turbine and electrolyzer for frequency stabilization in a microgrid system with plug-in hybrid electric vehicles," *Elect. Power Energy Syst.*, vol. 43, no. 1, pp. 804–811, 2012.
[21] S. Vachirasricirikul and I. Ngamroo, "Robust controller design of heat pump and plug-in hybrid electric vehicle for frequency control in a smart microgrid based on specified-structure mixed H_2/H_∞ control technique," *Appl. Energy*, vol. 88, no. 11, pp. 3860–3868, 2011.
[22] X. Li, Y.-J. Song, and S.-B. Han, "Frequency control in micro-grid power system combined with electrolyzer system and fuzzy PI controller," *J. Power Sources*, vol. 180, no. 1, pp. 468–475, 2008.
[23] V. P. Singh, S. R. Mohanty, N. Kishor, and P. K. Ray, "Robust *H*-infinity load frequency control in hybrid distributed generation system," *Int. J. Elect. Power Energy Syst.*, vol. 46, pp. 294–305, Mar. 2013.
[24] S. Vachirasricirikul and I. Ngamroo, "Robust LFC in a smart grid with wind power penetration by coordinated V2G control and frequency controller," *IEEE Trans. Smart Grid*, vol. 5, no. 1, pp. 371–380, Jan. 2014.
[25] S. Yang, Q. Lei, F. Z. Peng, and Z. Qian, "A robust control scheme for grid-connected voltage-source inverters," *IEEE Trans. Ind. Electron.*, vol. 58, no. 1, pp. 202–212, Jan. 2011.
[26] Y. Han, P. M. Young, A. Jain, and D. Zimmerle, "Robust control for microgrid frequency deviation reduction with attached storage system," *IEEE Trans. Smart Grid*, vol. 6, no. 2, pp. 557–565, Mar. 2015.
[27] A. Kahrobaeian and Y. A. I. Mohamed, "Direct single-loop μ-synthesis voltage control for suppression of multiple resonances in microgrids with power-factor correction capacitors," *IEEE Trans. Smart Grid*, vol. 4, no. 2, pp. 1151–1161, Jun. 2013.
[28] P. Li, Z. Yin, and Y. Li, "The realization of flexible photovoltaic power grid-connection μ-synthesis robust control in microgrid," in *Proc. IEEE PES Gen. Meeting Conf. Expo.*, National Harbor, MD, USA, 2014, pp. 1–5.
[29] M. J. Hossain, H. R. Pota, M. A. Mahmud, and M. Aldeen, "Robust control for power sharing in microgrids with low-inertia wind and PV generators," *IEEE Trans. Sustain. Energy*, vol. 6, no. 3, pp. 1067–1077, Jul. 2014.
[30] M. Babazadeh and H. Karimi, "A robust two-degree-of-freedom control strategy for an islanded microgrid," *IEEE Trans. Power Del.*, vol. 28, no. 3, pp. 1339–1347, Jul. 2013.
[31] D.-J. Lee and L. Wang, "Small-signal stability analysis of an autonomous hybrid renewable energy power generation/energy storage system part I: Time-domain simulations," *IEEE Trans. Energy Convers.*, vol. 23, no. 1, pp. 311–320, Mar. 2008.
[32] H. Bevrani, *Robust Power System Frequency Control*, 2nd ed. Gewerbestrasse, Switzerland: Springer, 2014.
[33] A. Packard and J. Doyle, "The complex structured singular value," *Automatica*, vol. 29, no. 1, pp. 71–109, 1993.
[34] D.-W. Gu, P. H. Petkov, and M. M. Konstantinov, *Robust Control Design With MATLAB*. New York, NY, USA: Springer, 2005.
[35] M. Morari and E. Zafirion, *Robust Process Control*. Englewood Cliffs, NJ, USA: Prentice-Hall, 1989.
[36] I. Pan and S. Das, "Kriging based surrogate modeling for fractional order control of microgrids," *IEEE Trans. Smart Grid*, vol. 6, no. 1, pp. 36–44, Jan. 2015.
[37] X. Tang *et al.*, "A novel frequency and voltage control method for islanded microgrid based on multienergy storage," *IEEE Trans. Smart Grid*, DOI: 10.1109/TSG.2014.2381235.
[38] R. Majumder, "Some aspects of stability in microgrids," *IEEE Trans. Power Syst.*, vol. 28, no. 3, pp. 3243–3252, Aug. 2013.

Hassan Bevrani (S'90–M'04–SM'08) received the Ph.D. degree in electrical engineering from Osaka University, Osaka, Japan, in 2004.

From 2004 to 2014, he was a Postdoctoral Fellow, a Senior Research Fellow, a Visiting Professor, and a Professor with Kumamoto University, Kumamoto, Japan; the Queensland University of Technology, Brisbane, Australia; the Kyushu Institute of Technology, Kitakyushu, Japan; Ecole Centrale de Lille, Lille, France, and Osaka University. Since 2000, he has been an Academic Member with the University of Kurdistan, Sanandaj, Iran. His current research interests include smart grid control, robust power system control, and microgrid control. He has authored four books, ten book chapters, and over 200 journal/conference papers.

Mohammad Ramin Feizi (S'14) was born in Sanandaj, Iran, in 1989. He received the B.Sc. degree from the Sahand University of Technology, Tabriz, Iran, in 2012, and the M.Sc. degree from the University of Kurdistan, Sanandaj, in 2014, both in electrical engineering.

He is currently a Lecturer with the Advanced Control Laboratory at the University of Kurdistan. His current research interests include micro/smart grids, and intelligent and robust control methods and their application in power system and power electronic industry.

Sirwan Ataee (S'14) was born in Kurdistan, Iran, in 1984. He received the B.Sc. degree from the Khajeh Nasir Toosi University of Technology, Tehran, Iran, in 2008, and the M.Sc. degree from Kurdistan University, Sanandaj, Iran, in 2014, both in electrical engineering.

His current research interests include renewable energy sources, power system operation and control, micro grids, and intelligent control.